scientific reports

Check for updates

OPEN

Optimized assay for transposase-accessible chromatin by sequencing (ATAC-seq) library preparation from adult *Drosophila melanogaster* neurons

Collin B. Merrill[1]✉, Miguel A. Pabon[2], Austin B. Montgomery[2], Aylin R. Rodan[2,3,4,5] & Adrian Rothenfluh[1,2,4,6]✉

Assay for transposase-accessible chromatin by sequencing (ATAC-seq) is rapidly becoming the assay of choice to investigate chromatin-mediated gene regulation, largely because of low input requirements, a fast workflow, and the ability to interrogate the entire genome in an untargeted manner. Many studies using ATAC-seq use mammalian or human-derived tissues, and established protocols work well in these systems. However, ATAC-seq is not yet widely used in *Drosophila*. Vinegar flies present several advantages over mammalian systems that make them an excellent model for ATAC-seq studies, including abundant genetic tools that allow straightforward targeting, transgene expression, and genetic manipulation that are not available in mammalian models. Because current ATAC-seq protocols are not optimized to use flies, we developed an optimized workflow that accounts for several complicating factors present in *Drosophila*. We examined parameters affecting nuclei isolation, including input size, freezing time, washing, and possible confounds from retinal pigments. Then, we optimized the enzymatic steps of library construction to account for the smaller *Drosophila* genome size. Finally, we used our optimized protocol to generate ATAC-seq libraries that meet ENCODE quality metrics. Our optimized protocol enables extensive ATAC-seq experiments in *Drosophila*, thereby leveraging the advantages of this powerful model system to understand chromatin-mediated gene regulation.

Assay for transposase-accessible chromatin by sequencing (ATAC-seq) is a relatively new technique that has advanced our understanding of chromatin-mediated gene regulation. The technique offers several advantages over other sequencing techniques that examine chromatin, such as DNase-seq, micrococcal nuclease (MNase-seq), or formaldehyde-assisted isolation of regulatory elements (FAIRE-seq), including low input requirements (50,000–60,000 nuclei vs. 50 million nuclei for DNase-seq or 1–10 million nuclei for MNase- or FAIRE-seq)[1–3], less hands-on time, no harsh chemicals such as paraformaldehyde, and no antibody optimization or complicated pull-down methods. ATAC-seq is also robust to small sample sizes and has been adapted for single-cell applications[4,5]. Thus, ATAC-seq is quickly becoming the assay of choice for chromatin studies.

ATAC-seq was developed using peripheral blood samples[6], and many studies using ATAC-seq focus on mammalian or human-derived tissues[7–9]. Recent studies used ATAC-seq to investigate other tissue types, including tissues from plants[10], zebrafish[11], and livestock[12]. Some ATAC-seq studies using *Drosophila melanogaster* have

[1]Department of Psychiatry, Huntsman Mental Health Institute, University of Utah, Salt Lake City, UT 84108, USA. [2]Molecular Medicine Program, University of Utah, Salt Lake City, UT 84112, USA. [3]Division of Nephrology and Hypertension, Department of Internal Medicine, University of Utah, Salt Lake City, UT 84112, USA. [4]Department of Human Genetics, University of Utah, Salt Lake City, UT 84112, USA. [5]Medical Service, Veterans Affairs Salt Lake City Health Care System, Salt Lake City, UT 84148, USA. [6]Department of Neurobiology, University of Utah, Salt Lake City, UT 84112, USA. ✉email: collin.merrill@utah.edu; adrian.rothenfluh@hsc.utah.edu

been published, though many of these studies focus on embryogenesis and larvae[13–15]. One recent report performed ATAC-seq from central brains after fluorescent sorting of GFP-positive cell bodies[16]. However, the physical dissection and dissociation of many brains can be labor-intensive and yield relatively few cells, in that case 6000–10,000 cells[16]. We were interested in optimizing the standard ATAC-seq protocol to allow efficient library preparation while taking advantage of the many genetic tools available for labeling specific *Drosophila* neurons[17].

ATAC-seq library preparation has several parameters that can be optimized based on the input tissue. Many of these parameters are addressed in the original ATAC-seq protocol[6]. Additional studies optimized ATAC-seq library preparation from various tissue types in several storage conditions[18–21]. Most studies in *Drosophila* larvae treat the tissue similarly to mammalian tissues, only adding an additional washing step to clean the embryos or larvae before homogenization[14,22]. ATAC-seq library preparation using adult *Drosophila* poses challenges that are not present in other tissues. For example, the insect cuticle is a chitin structure that is difficult to process by simple homogenization. Another challenge is eye color, which is commonly used to identify the presence of transgenic insertions, and many transgenic fly lines contain the *mini-white* (w^{+mC}) gene. In a w^- background, *mini-white* confers a yellow to red eye color, so eye color can range from white (w^-) to red, depending on the genotype. Some *Drosophila* retinal pigments emit fluorescence[23,24] that can complicate fluorescent-activated nuclei sorting (FANS). Finally, the *Drosophila* genome is considerably smaller than mammalian genomes[25,26], so established ATAC-seq parameters may use higher-than-optimal enzyme concentrations and long incubation times that may lead to low-quality ATAC-seq libraries when prepared from fly tissues. Thus, optimizing each parameter for ATAC-seq library preparation using adult flies should be performed prior to sequencing. However, these experiments add considerable sequencing costs, putting the approach out-of-reach for many labs.

Identifying cell- and tissue-specific roles in organism function is a major goal of many current studies, which require specific and sensitive detection of target cells, especially for rare cell types. To facilitate these studies, we developed a protocol to generate ATAC-seq libraries from adult *Drosophila* neurons. Our goal was to optimize each variable in the library preparation process, with particular attention to challenges specific to *Drosophila* model systems. Our protocol provides guidelines for ATAC-seq library preparation using *Drosophila* and outlines the optimal parameters for each library preparation step. This protocol will accelerate studies of chromatin-mediated gene regulation in flies by coupling the powerful genetic tools in *Drosophila* with high-throughput, in-depth examination of chromatin structure.

Materials and methods

Fly strains. The following fly lines were obtained from the Bloomington Drosophila Stock Center (Indiana University, Bloomington, IN, USA) and used in this study: *Canton S* (BL64349), *tub-Gal4* (BL5138), *elav-Gal4* (BL458), *nSyb-Gal4* (BL51635) *UAS-GFP-nls* (encoding green fluorescent protein with a nuclear localization signal; BL4775), *UAS-Stinger* (a super-bright GFP-nls variant; BL84277), *TH-Gal4* (BL8848), *Cha-Gal4.19B* (BL6798), and *vGAT-Gal4* (BL58980). *w* Berlin* flies have been in the lab for many generations[27] and were originally a gift from Martin Heisenberg. Flies were reared in bottles containing standard cornmeal agar and grown at 25 °C with 70% relative humidity and a 12-h light/dark cycle.

Nuclei isolation. All equipment and buffers were pre-chilled to be ice-cold. All plastic and glassware used for nuclei isolation was pre-treated with 1% bovine serum albumin (BSA) in phosphate-buffered saline (PBS). Flies were collected into empty bottles and frozen at − 80 °C. Then, the flies were placed in pre-chilled (in a − 80 °C freezer) sieves and agitated for 1 min to separate the heads from the bodies. The fly heads were added to lysis buffer [10 mM Tris–HCl pH 7.5, 10 mM NaCl, 3 mM $MgCl_2$, 0.1% Tween-20, 0.1% Nonidet P40 substitute, 0.01% digitonin (ThermoFisher Scientific, Waltham, MA, USA), and 1% bovine serum albumin] in a Dounce homogenizer. The tissue was homogenized with the A pestle until the resistance disappeared. The crude homogenate was passed through a 40 µm filter and homogenized with 15 slow strokes with the B pestle. The crude nuclei were washed with wash buffer (10 mM Tris–HCl, 10 mM NaCl, 3 mM $MgCl_2$, 1% BSA, and 0.1% Tween-20) and centrifuged at 500*g* for 10 min per wash. The washed nuclei were resuspended in 1 mL wash buffer with 3 mM DAPI for evaluation and sorting.

Fluorescence-activated nuclei sorting (FANS). Nuclei were evaluated and sorted with a BD FACS Aria flow cytometer (BD Biosciences, San Jose, CA, USA) operated by the University of Utah Flow Cytometry Core facility. Nuclei collected from *w* Berlin* flies (no GFP) were stained with 3 µM DAPI and used as the GFP-negative control to set the sorting gates. GFP-positive nuclei were collected into 500 µL wash buffer and stored on ice until use for ATAC-seq library prep. Nuclei counts were determined using an internal control bead population (Spherotech, Lake Forest, IL, USA) at 10^6 beads/mL. Briefly, 20 µL of well-mixed beads were added to 200 µL of nuclei suspension and gently mixed. Data was recorded for the bead and cell mixture until at least 10,000 singlet beads were collected. Nuclei were identified based on the forward scatter signal and DAPI intensity. The number of nuclei was calculated as follows: number of nuclei recorded × 10^5/number of beads recorded = number of nuclei/mL.

DNA tagmentation, amplification, and purification. Purified nuclei were centrifuged for 10 min at 500*g* at 4 °C. The pellet was mixed with 22.5 µL 2× Tn5 tagmentation buffer [20 mM Tris–HCl pH 7.6, 10 mM $MgCl_2$, and 20% dimethyl formamide (Sigma Aldrich, St. Louis, MO, USA) in sterile water], 16.5 µL 1× PBS, 0.5 µL Tween-20, 5.5 µL water, and Tn5 enzyme (Illumina, Inc., San Diego, CA, USA). The mixture was incubated at 37 °C for various times and the DNA was purified using a MinElute PCR purification kit (Qiagen, Germantown, MD, USA). Then, the purified DNA was mixed with CD index primers (Illumina) and Phusion High Fidelity PCR MasterMix (New England Biolabs, Ipswich, MA, USA) and was amplified by 1 cycle of 72 °C

for 5 min and 98 °C for 30 s, followed by 5 cycles of 98 °C for 10 s, 63 °C for 30 s, and 72 °C for 1 min in a C100 thermocycler (BioRad, Hercules, CA, USA). 5 µL of this reaction was removed and used for a qPCR side reaction. The aliquot was mixed with the same CD index primers and SsoFast EvaGreen Supermix (BioRad) and amplified for 1 cycle of 98 °C for 30 s and 40 cycles of 98 °C for 10 s, 63 °C for 30 s, and 72 °C for 1 min in an Applied Biosystems 7900HT qPCR instrument (ThermoFisher Scientific). Total fluorescence was calculated from the background-subtracted maximum fluorescence of each sample. The cycle number corresponding to a portion of the total fluorescence was determined (~ 8–10 cycles) and the DNA was amplified for this number of additional cycles. After amplification, the DNA was purified with 0.5× and 1.1× AMPure XP beads (Beckman Coulter, Indianapolis, IN, USA) to remove primer-dimers and high-molecular weight DNA (> 5000 bp). The purified DNA was stored at − 20 °C until further analysis.

ATAC-seq library quality assessment. ATAC-seq library quality was assessed using an Agilent 2200 TapeStation and High Sensitivity D5000 ScreenTape assays (Agilent Technologies, Inc., Santa Clara, CA, USA) at the Huntsman Cancer Institute High Throughput Genomics core facility or the Genome Technology Access Center of the McDonnell Genome Institute at the Washington University School of Medicine (St. Louis, MO, USA).

Next generation sequencing and analysis. ATAC-seq libraries constructed using nuclei isolated from dopaminergic and GABAergic neurons were sequenced on a Novaseq 6000 instrument (Illumina) using 50-bp paired-end reads. The sequencing data was analyzed as previously described[28]. Briefly, Fastq files were quality checked using FastQC (v 0.11.9). Adapter sequences were removed with CutAdapt (v3.4). The sequenced reads were aligned to the dmel_r6.26 genome assembly using Bowtie2 (v2.4.2; Langmead and Salzberg[29]). Aligned reads were sorted with Samtools (v1.12; Li et al.[30]) and deduplicated with Picard (v2.23) using the MarkDuplicates command. Aligned, filtered, and deduplicated reads were used to call peaks using MACS2 software (v2.2.5; Zhang et al.[31]). Then, featureCounts (v2.6.4; Liao et al.[32]) was used to generate the count matrix. Differential accessibility analysis was performed using DESeq2 (v1.32.0; Love et al.[33]). Insert size distributions were calculated using Picard. Peaks were visualized using the IGV browser (v2.7.2).

Statistical analysis. The data are represented as means ± standard deviation. Comparisons between homogenizer size and fly volume were analyzed by two-way ANOVA with Bonferroni's multiple comparison tests. Freezing time was analyzed by one-way ANOVA using Tukey's multiple comparison tests. Eye color experiments, % read alignment, and fractions of reads in peaks (FRiP) were analyzed using Student's t-tests. Gal4-UAS and washing experiments were analyzed by simple linear regression, and analysis of covariance (ANCOVA). All statistical analyses were performed using GraphPad Prism 9 software (San Diego, CA, USA).

Results

Sample volumes, homogenization, and freezing time. Our goal was to identify the optimal conditions for nuclei isolation, purification, and ATAC-seq library preparation using adult *Drosophila*. We first asked if the number of flies used for head isolation and the size of the Dounce homogenizer play a role in the number of extracted nuclei that are labeled with DAPI. Using a larger volume of flies increased the number of extracted nuclei (2-way ANOVA, $F(1,8) = 15.6$, $p = 0.004$). The size of the Dounce homogenizer used for extraction did not significantly affect the total extracted nuclei if analyzed by 2-way ANOVA ($F(1,8) = 2.0$, $p = 0.20$; Fig. 1a), however, with 0.5 mL of flies, more nuclei were isolated with the 7 mL homogenizer (significant by isolated t-test). Thus, we recommend using the larger, 7 mL Dounce homogenizer to maximize nuclei extraction.

One advantage to using *Drosophila* is the availability of sophisticated genetic tools that allows the easy identification of target cells, which can then be isolated by flow cytometry. In our nuclei isolation procedure, live *neuronal synaptobrevin* (*nSyb*)*-Gal4* flies expressing pan-neuronal GFP-nls are frozen at − 80 °C for 5 min, which is similar to slow freezing, since the flies are not immediately frozen when placed in the freezer, as would occur when snap-freezing in liquid nitrogen. Snap-freezing can decrease GFP fluorescence[34] and damage neurons[19,35], thus decreasing the number of viable GFP-positive nuclei collected by flow cytometry. We hypothesized that extended freezing at − 80 °C could reduce GFP fluorescence or nuclear viability, so we performed a time-course experiment to examine whether freezing time influences the detection of GFP-positive nuclei by flow cytometry. Five minutes is about the minimum time per sample in which flies can be frozen at − 80 °C and homogenized when handling multiple samples. We observed that GFP fluorescence decreased quickly with additional time on dry ice but reached a plateau at ~ 60% fluorescence in the time analyzed (Fig. 1b, one-phase exponential decay, $K = 0.51\ min^{-1}$, goodness of fit $R^2 = 0.64$). Therefore, we suggest that flies should only be frozen briefly (5 min or less) at − 80 °C when used for nuclei isolation and ATAC-seq library preparation.

Flow cytometer specificity and sensitivity. ATAC-seq is prone to mitochondrial DNA contamination[6,18], which reduces the number of reads aligning to the nuclear genome. Since *Drosophila* can be used to easily label target nuclei, fluorescence-activated nuclei sorting is a convenient way to isolate nuclei of interest while simultaneously reducing mitochondrial contamination. Sorting GFP+ nuclei using a flow cytometer is dependent on the gating scheme for the detection of green fluorescent signal. Detection schemes for stains usually come at a low gate (less signal required) and a high gate (more signal required). To determine the sorting sensitivity at these gates, we ubiquitously expressed a brighter version of nuclear GFP, *UAS-Stinger*, using a strong *Tubulin-Gal4* driver. At the low gate, we recovered ~ 80% of nuclei from ~ 100,000 DAPI+ nuclei (Fig. 2a,b), while we recovered ~ 12% of nuclei with the high gate (Fig. 2c,d). The data from these experiments suggest that the low gate has six- to seven-fold better sensitivity than the high gate.

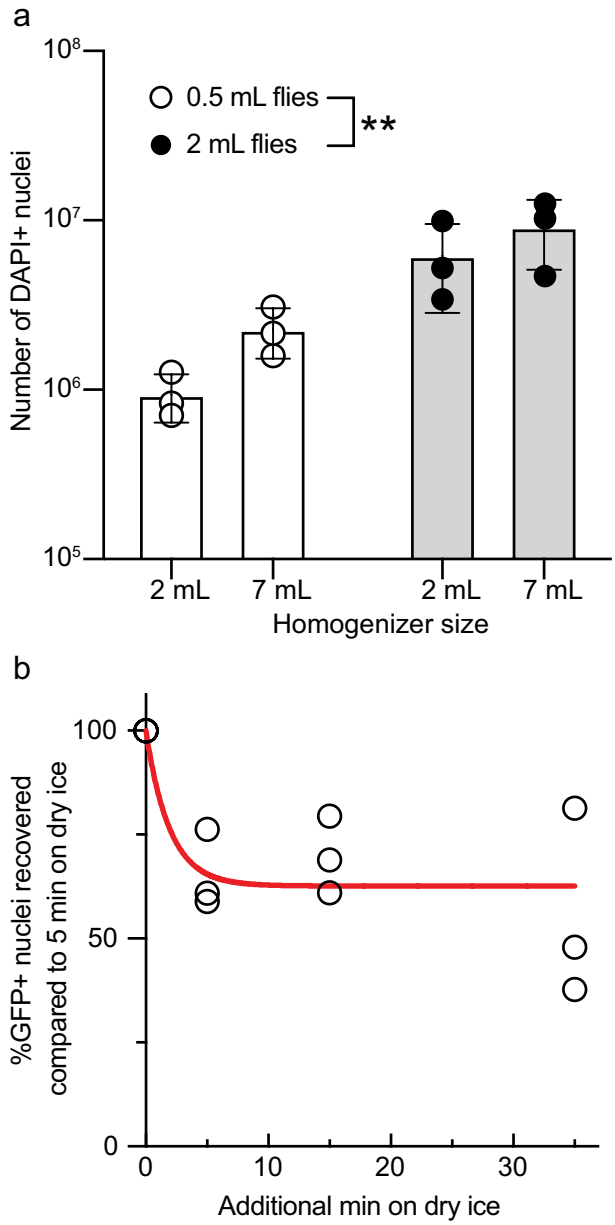

Figure 1. Sample volume and freezing time affect nuclei yield. (**a**) The number of flies used to collect heads prior to nuclei isolation increases the number of extracted nuclei, but the homogenizer size does not. The indicated volumes of *w* Berlin* flies were used for nuclei isolation. Data represent the mean ± SD of three independent experiments. (**b**) Freezing time longer than 5 min decreases GFP detection by flow cytometry. Flies expressing pan-neuronal GFP (*nSyb-Gal4 UAS-GFP-nls*) were counted at the low gate. Data represent three biological replicates. The data in (**a**) were analyzed by two-way ANOVA and the data in (**b**) were analyzed by nonlinear regression using one-phase exponential decay, K = 0.51 min^{-1}, goodness of fit $R^2 = 0.64$. $^{**}p < 0.01$.

To examine the sorting specificity, we evaluated the number of sorted 'GFP+ nuclei' in *w* Berlin* flies, which are all GFP-negative. Sorting at the low gate yielded 0.093% 'GFP+' nuclei (Fig. 3a), while at the high gate, 0.026% of nuclei were 'GFP+' (Fig. 3b). Together, these data suggest that the high gate has fourfold higher specificity and is better at calling true positives. As expected, there is a tradeoff between sensitivity and specificity when using low and high GFP+sorting gates.

Drosophila-specific parameters affect nuclei isolation. Using the high sorting gate, 1 in ~ 4000 nuclei are selected as false-positive. At face value, this is good specificity. However, assuming that a *Drosophila* head contains > 200,000 nuclei, > 50 of those will be sorted as false positives at the high gate (and > 200 at the low gate). These numbers would significantly contaminate the nuclei sorted from a genotype where Gal4 is expressed in a subset of only hundreds of neurons. The high gate will produce fewer false positives, thus increasing the

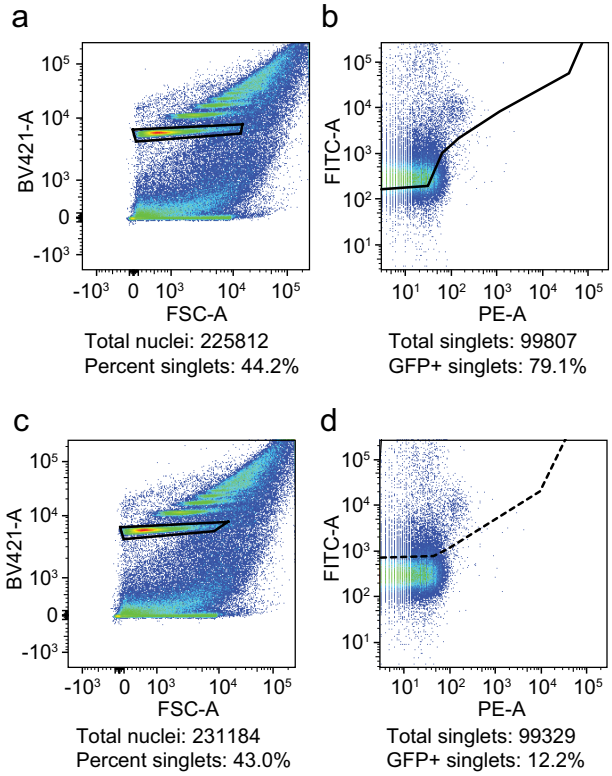

Figure 2. Differential sensitivity at the low and high sorting gate. Super-bright nuclear GFP expression was driven using *tubulin-Gal4* (all nuclei are GFP+). Nuclei from heads were isolated and analyzed by flow cytometry using low- and high-stringency gating. (**a**) 79% of nuclei were GFP+ at the low gate (solid trapezoid). (**b**) 12% of nuclei were GFP+ at the high gate (stippled trapezoid). The left panels show forward scatter vs. DAPI staining and the right panels show GFP fluorescence.

specificity for the Gal4-expression pattern, but the high gate will also reduce the sensitivity and recovery of those Gal4 + neurons. Therefore, we asked whether we could increase the recovery via genetic means by increasing the number of *Gal4* or *UAS-GFP-nls* transgenic constructs to boost GFP expression. We used *ics-Gal4 UAS-GFP-nls* flies and crossed them to themselves, *ics-Gal4*, *UAS-GFP-nls*, or *w* Berlin* to generate flies with 4, 3, 3, or 2 combined copies of *Gal4/UAS* insertions, respectively. *ics-Gal4* expression includes many neurons and the expression pattern is not different between *ics-Gal4/+* hetero- and *ics-Gal4* homozygotes[36]. Expanding the copies of *Gal4/UAS* insertions increased the number of detected GFP+ nuclei (linear regression, slope ≠ 0, $p = 0.0008$, low gate; $p = 0.001$, high gate, Fig. 4a). At both gates, the recovery with 4 transgenes was about 20-fold higher than recovery with 2 transgenes. We therefore recommend that for Gal4-lines with sparse expression patterns, the amount of GFP produced should be increased genetically.

Most *Drosophila* transgenic insertions are marked with a miniature copy of the *white*$^{+}$ gene, w^{+mC}. The presence of such a transgene will confer anywhere from pale yellow to red-colored eyes. In addition, the allele w^{+mC} is dosage-sensitive, i.e. the more transgenes in the fly labeled with w^{+mC}, the closer to wild-type red the eye color will be. Since we suggested above that increasing the copy of *Gal4* and/or *UAS* transgenes will increase the recovery of GFP+ nuclei, we next wanted to determine if red-colored eye pigment interferes with sorting GFP+ nuclei. We crossed w^{-}*;Cha-Gal4 UAS-GFP-nls* males to white-eyed (w^{-}), or to red-eyed (w^{+}) virgins and then collected the male progeny. Both of these male genotypes contain 2 w^{+mC} alleles from the transgenes, but one group is wild-type red-eyed (w^{+}) and the other is orange-eyed (in a w^{-} background). At the low gate, we recovered almost twice as many 'GFP+ nuclei' (Fig. 4b), suggesting that red eye pigment from w^{+} contributes to the false positive rate. We hypothesized that increasing the number of washes during nuclei isolation would mitigate the false positive rate caused by red eye pigments. Washing the crude nuclei extracts one, three-, or five-times dose-dependently reduced the GFP+/DAPI+ ratio in red-eyed and orange-eyed flies. For the red-eyed flies, we observed the steepest decrease between one and three washes, and with three washes, there was no longer a difference in the GFP+/DAPI+ ratio between red- and orange-eye flies (Fig. 4c,d). We therefore recommend at least three washes, especially when sorting with the low-stringency gate and as more w^{+mC}-marked transgenes are used, since the eye color will approach wild-type red.

Reaction conditions affect library quality. Published ATAC-seq guidelines are based on mammalian genomes, which are approximately tenfold larger than the *Drosophila* genome[25,26]. Therefore, the parameters used for the Tn5 transposition reaction (incubation time and enzyme concentration) in mammalian cells may not be appropriate for fly nuclei. To determine the optimal Tn5 reaction conditions, we sorted GFP+ nuclei from

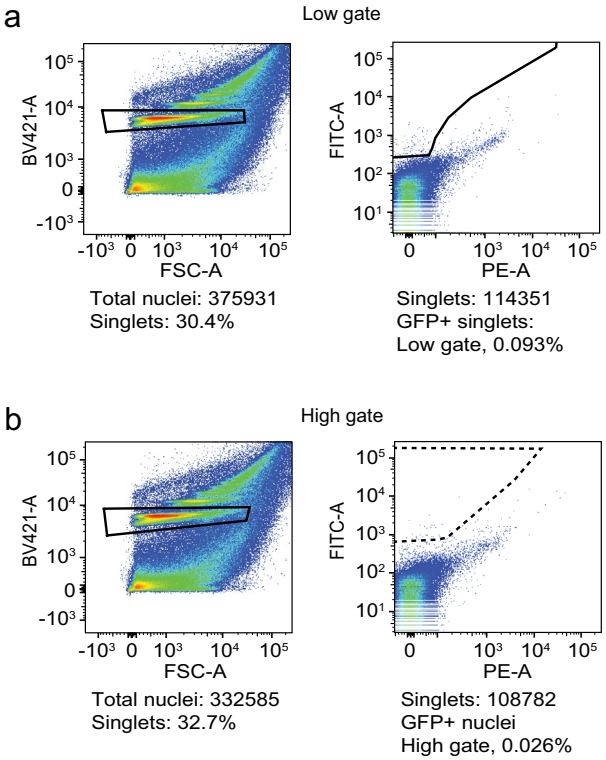

Figure 3. Flow cytometry shows high specificity and few false positives. Nuclei were isolated from *w* Berlin* heads (GFP-negative) and analyzed by flow cytometry. (**a**) Representative dot plots of nuclei analyzed using the low gate. Nuclei were identified by DAPI staining (Y-axis) and forward light scatter (X-axis, left). The box indicates the sorted DAPI+ singlet nuclei, which were then analyzed for green fluorescence (Y-axis) and the red PE-A channel (X-axis, right), which allowed the best separation of GFP populations. The nuclei were sorted at the low gate (solid trapezoid box). 0.093% of input singlets were GFP false-positives (and 0.024% when applying the high gate in this sort). (**b**) Representative dot plots of nuclei analyzed using the high gate. Nuclei were isolated as in (**a**) and sorted for green fluorescence at the high gate (stippled trapezoid box, right). 0.026% of input singlets were GFP false-positives (and 0.10% when applying the low gate in this sort).

fly heads and constructed ATAC-seq libraries. We evaluated the library quality using the guidelines recommended by Buenrostro et al.[37]. We first examined how reaction time affects the fragment distribution by sorting pan-neuronal GFP+ nuclei from *nSyb-Gal4 UAS-GFP-nls* fly heads. Then, we prepared ATAC-seq libraries using 1× Tn5 enzyme and sample incubation for 5, 23, and 60 min (Fig. 5a). A low reaction time decreased the nucleosome-free peak and increased the proportion of larger fragments up to 1000 bp, suggesting that di-, tri- and multi-nucleosome fragments are over-represented. Incubation for 23 min provided a fragment distribution with more nucleosome-free and fewer mono- and di-nucleosome fragments, while increasing the reaction time to 60 min biased the library toward smaller fragment sizes with relatively little evidence of larger fragments. Thus, for library preparation using *Drosophila* nuclei, 23 min is the optimal reaction time. We next examined how the Tn5 concentration affects libraries by collecting GFP+ nuclei from *tubulin-Gal4 UAS-stinger-nls* flies and tagmenting the DNA using 0.1×, 0.3×, 1×, and 3× Tn5 (compared to manufacturer recommendation; Fig. 5b). 1× Tn5 showed the largest peak around 200 bp, with additional skewing towards larger fragments. Reacting DNA using 3× Tn5 reduced both skewness toward larger fragments and the number of nucleosome-free fragments due to over-digestion of DNA [which was size-filtered (150–2000 bp) before analysis, Fig. 5b]. Reducing the Tn5 concentration to 0.1× showed skewness to higher fragments, but overall fewer amplified fragments and reduced overall recovery. We therefore recommend 1× Tn5 as the best balance between recovery of amplified fragments and avoiding over-digestion. Finally, we examined how library amplification affects quality. Like other sequencing library types, ATAC-seq libraries must be amplified to obtain sufficient DNA concentrations for sequencing. Buenrostro et al.[6,37] suggested that ATAC-seq libraries should be amplified to 33% of maximal fluorescence obtained in a qPCR pre-reaction to ensure that sufficient material is present for sequencing, without the introduction of GC and size bias. We hypothesized that the smaller genome size in *Drosophila* would require more PCR cycles than libraries derived from mammalian nuclei. We tagmented DNA from pan-neuronal GFP+ nuclei from *nSyb-Gal4 UAS-GFP-nls* fly heads with 1X Tn5 and amplified the tagmented DNA to 25%, 33%, and 50% total fluorescence in a qPCR side reaction (40 cycles) to determine the number of PCR cycles needed for library amplification before sequencing (Fig. 5c). The library that was amplified to 33% total fluorescence had the smallest amount of nucleosome-free fragments and a large proportion of ~800–1200 bp fragments, which may correspond to a PCR bubble that arose from depleted PCR reagents, most likely primers[38]. In contrast, the library

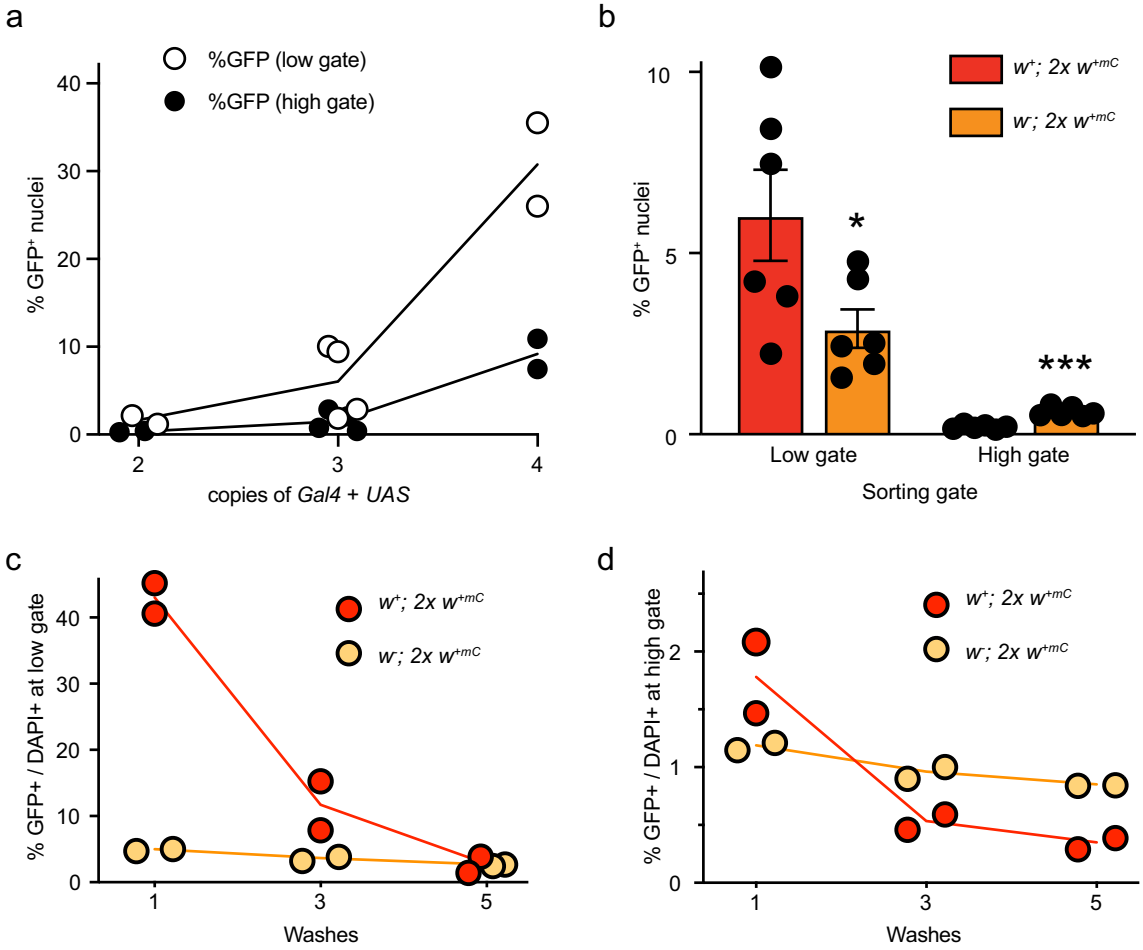

Figure 4. Physical parameters affecting ATAC-seq library preparation from *Drosophila* nuclei. (**a**) GFP+ nuclei from flies expressing multiple copies of Gal4 + UAS (*ics-Gal4 UAS-GFP-nls*) were isolated and analyzed by flow cytometry using low- and high-stringency gating. (**b**) Nuclei from cholinergic neurons (*Cha-Gal4 UAS-GFP-nls*) in red-eyed (w^+ background) and orange-eyed flies (w^- background). Error bars represent the mean ± SD of six biological replicates and were analyzed by Student's t-tests. (**c**,**d**) Nuclei from the same flies used in (**b**) were washed multiple times before analysis using low- (**c**) and high- (**d**) stringency gating. The data were analyzed using linear regression. All regression lines have slopes ≠ 0, $p < 0.02$.

amplified to 25% total fluorescence showed a broad nucleosome-free peak and an even distribution of higher molecular weight fragments, while the library amplified to 50% total fluorescence showed a tall nucleosome-free peak that suggests a bias toward low molecular weight amplification. These results suggest that ATAC-seq libraries derived from *Drosophila* nuclei should be amplified to 25% of total qPCR fluorescence, though 33%-amplified libraries may also be suitable for sequencing after reconditioning PCR[39].

Optimized reaction conditions generate ATAC-seq libraries conforming to ENCODE standards. Finally, we combined our optimized parameters (Supplementary File 1) to generate and sequence ATAC-seq libraries. We drove nuclear GFP expression in dopaminergic and GABAergic neurons and isolated the nuclei after freezing approximately 1 mL (300–400) flies at − 80 °C for 5 min. The crude nuclei extracts were washed three times and sorted by flow cytometry using a high-stringency gate. We collected 65,000 nuclei per sample for each neuron type, which were tagmented for 23 min using 1× Tn5. The resulting libraries were amplified to 25% qPCR fluorescence and analyzed using 50-bp paired end sequencing. We then examined the percent alignment to the genome, the fraction of reads in peaks (FRiP), and fragment length distribution of the sequenced libraries. Both libraries showed high alignment rates, with 79% and 94% alignment in dopaminergic and GABAergic libraries, respectively ($p = 0.2$; Fig. 6a). Dopamine neuron libraries had 0.37 FRiP, while GABA neuron libraries had 0.40 FRiP ($p = 0.8$; Fig. 6b), which were both higher than the FRiP values (> 0.3) recommended by the ENCODE consortium for ATAC-seq libraries[40]. Finally, each of these libraries showed the expected nucleosomal banding pattern (Fig. 6c). Together, these metrics were similar to those observed in other ATAC-seq studies using adult *Drosophila*[16], which indicates that we generated high-quality libraries and that our protocol returns high-quality sequencing data. To test this hypothesis, we examined ATAC-seq peaks in regions associated with classical neuron markers identified by single-cell RNA-seq[41]. We observed dif-

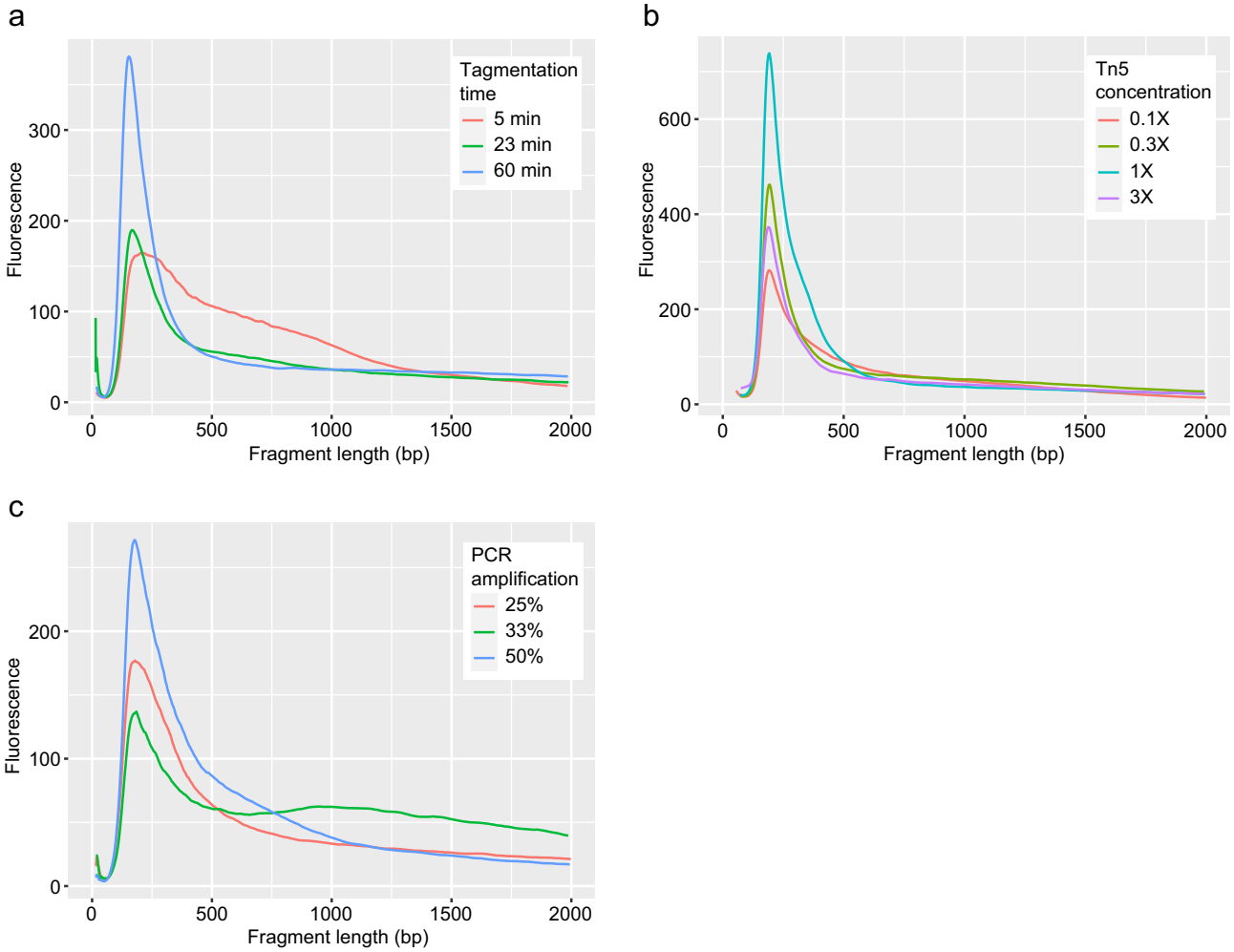

Figure 5. Optimal library construction parameters. Nuclear GFP expression was driven using various genotypes. Isolated nuclei were used in ATAC-seq library construction. The fragment sizes and relative fluorescence from Tapestation data are shown. (**a**) Tn5 reaction time; (**b**) Tn5 concentration; and (**c**) post-Tn5 PCR amplification. GFP expression was driven using (**a**,**c**) *nSyb-Gal4 UAS-GFP-nls* or (**b**) *tubulin-Gal4 UAS-Stinger.*

ferential peaks indicating increased accessibility in *ple*, *DAT*, and *hth*, which encode tyrosine hydroxylase, the rate-limiting dopamine-synthesis enzyme, dopamine transporter, and homothorax, a dopaminergic-enriched homeobox transcription factor[42], respectively. These peaks were significantly more open in dopamine neurons than in GABA neurons [peaks indicated by numbers in Fig. 7a; *ple*: $p = 3.32e{-}65$ (1) and 5.01e−53 (2); *DAT*: $p = 1.03e{-}05$ (3) and 1.04e−05 (4); *hth*: $p = 0.009$ (5), 1.69e−36 (6), and 1.14e−21 (7)]. Peaks associated with dopamine-neuron specific genes were much smaller or absent in GABA neurons (Fig. 7a). The peaks corresponding to known GABAergic markers[41] include *Gad1*, which encodes glutamic acid decarboxylase, which synthesizes GABA, *Lim3*, and *CG14989*. Peaks associated with GABA marker genes were significantly more open in GABA neurons than in dopamine neurons [peaks indicated by numbers in Fig. 7b; *GAD1*: $p = 0.0005$ (1), 4.42e−08 (2), 0.04 (3), 0.01 (4), and 6.6e−08 (5); *Lim3*: $p = 1.39e{-}05$ (6) and 0.001 (7); *CG14989*; $p = 0.1$]. These peaks were much smaller or absent in dopaminergic neurons. These results confirm that our nuclei isolation and library generation protocol yields high quality data, including differential chromatin accessibility in known cell-type markers[41].

Discussion

Previous studies using ATAC-seq focused on either tumor tissue or white blood cells, though recent studies have investigated the brain and other tissues in mice and humans[7,43]. The initial study describing ATAC-seq was performed in mammalian tissue[6], and published protocols have been optimized for use in these tissues[5,18]. *Drosophila melanogaster* is a powerful model organism that is routinely used to study development and human disease models. Because we are interested in *Drosophila* neurons from the adult brain, we first determined some basic parameters for nuclei isolation. Briefly freezing flies does not reduce GFP+ fluorescence, but longer freezing reduced GFP+ nuclei recovery. Using adult *Drosophila*—heads or whole flies—for ATAC-seq experiments presents some complicating factors, such as the exoskeleton. While brains can be manually dissected, we used

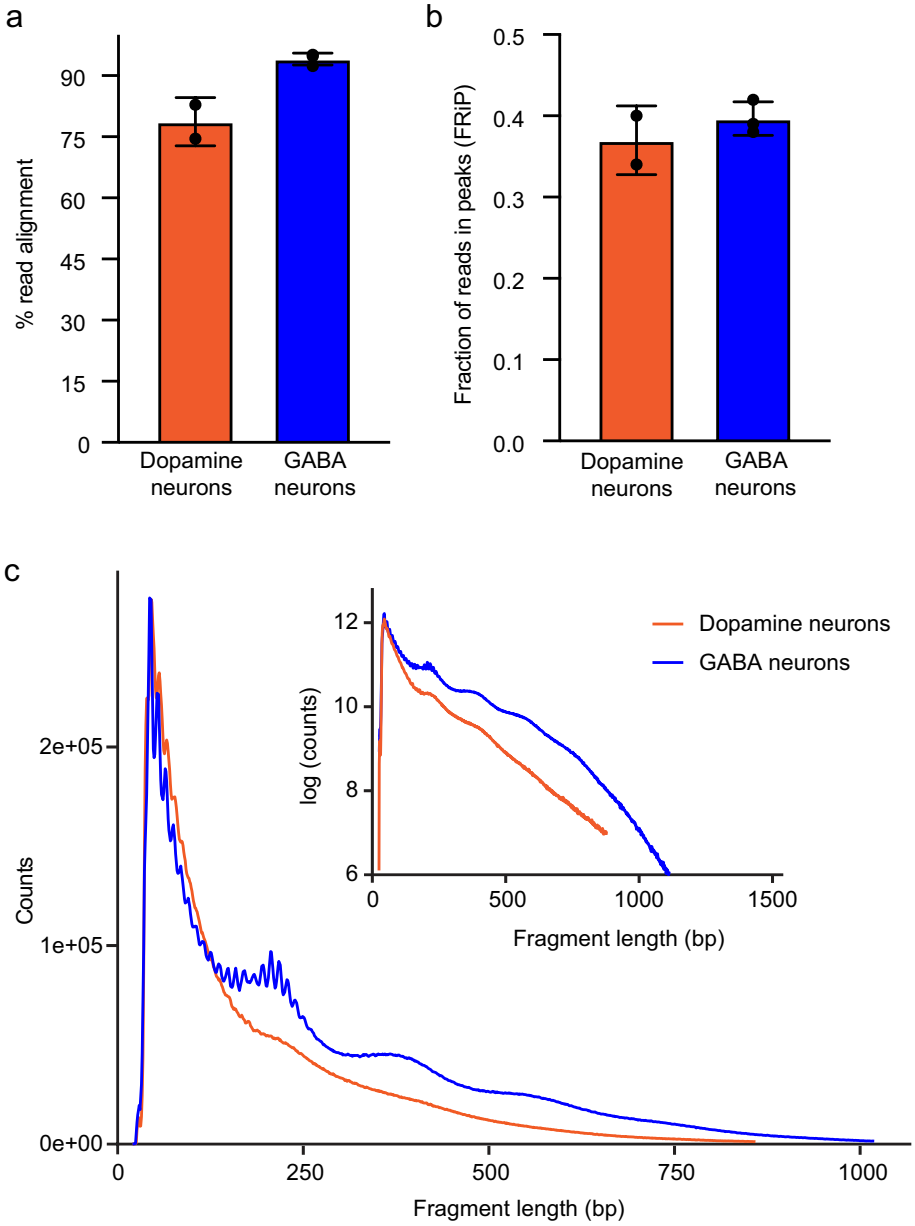

Figure 6. Optimized ATAC-seq parameters generate consistent libraries. Representative traces from ATAC-seq libraries prepared from dopaminergic and GABAergic nuclei isolated from adult *Drosophila* heads. The libraries were prepared using GFP+ nuclei from *TH-Gal4* (dopamine) and *vGAT-Gal4* (GABA) flies using our optimized protocol. (**a**) Fraction of reads uniquely aligned to the nuclear genome. The alignment rates were not significantly different between libraries prepared from dopaminergic and GABAergic neurons ($p = 0.2$). (**b**) Fraction of reads in peaks (FRiP) after alignment, filtering, and peak calling. The FRiP values were not significantly different between the libraries ($p = 0.8$). (**c**) Insert size distribution showing the expected nucleosomal periodicity. Inset: Log-scaled insert size distribution. In (**a**) and (**b**), the data represent the mean ± SD of at least two replicates per neuron type. Statistical differences were analyzed using Mann–Whitney U tests.

undissected heads for nuclei isolation, which provides more efficient throughput and sufficient GFP+ nuclei from populations of few neurons. We homogenized and filtered the homogenate, which eliminated exoskeletal debris, while the lysis buffer disrupted the plasma membrane without disrupting the nuclear membrane[18]. Our isolation procedure allowed us to recover up to 80% of GFP+ nuclei. Thus, our physical extraction protocol allows for efficient and sensitive recovery of GFP-labelled nuclei from adult *Drosophila* heads.

An advantage of using *Drosophila* for ATAC-seq studies is the ability to genetically label nuclei of interest using the *Gal4/UAS* system. Thousands of Gal4 lines labeling distinct neurons are available[17], including ones specific to neurotransmitters[44], allowing for the specific, reproducible interrogation of only a defined subset of neurons. For ATAC-seq, we recommend flies expressing GFP tagged with a nuclear localization signal, since this

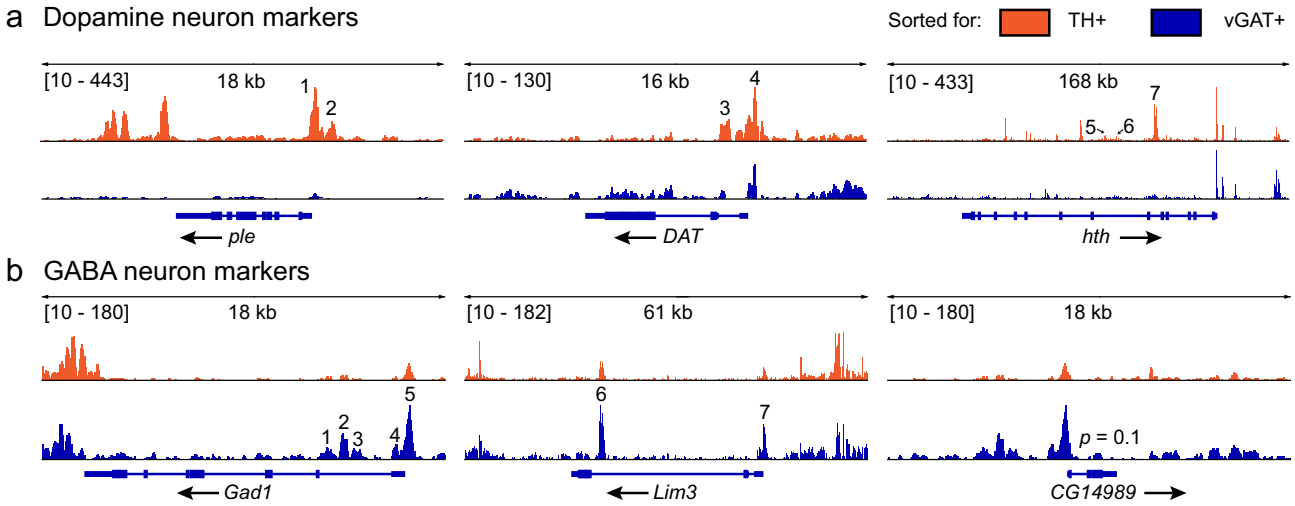

Figure 7. Optimized ATAC-seq libraries return expected cellular markers. ATAC-seq peaks in marker genes for dopaminergic and GABAergic neurons. ATAC-seq reads from dopamine neurons (tyrosine hydroxylase: TH+) are shown in orange and reads from GABA (vesicular GABA transporter: vGAT+) neurons are shown in blue. The genes and gene structures are shown below the ATAC-seq peaks. (**a**) Peaks in chromatin regions that are more open in dopamine neurons. *ple* (encoding tyrosine hydroxylase; $p = 2.43e{-}68$) and *DAT* (dopamine transporter; $p = 9.64e{-}7$) are classical dopamine neuron markers. *hth* (homothorax; $p = 1.16e{-}52$) is a recently described dopamine neuron marker. *ple*: $p = 3.32e{-}65$ (1) and $5.01e{-}53$ (2); *DAT*: $p = 1.03e{-}05$ (3) and $1.04e{-}05$ (4); *hth*: $p = 0.009$ (5), $1.69e{-}36$ (6), and $1.14e{-}21$ (7). (**b**) Chromatin regions that are more open in GABA neurons. *Gad1* (glutamic acid decarboxylase 1; $p = 6.64e{-}8$) is a classical GABAergic neuron marker, while *Lim3* (Lim3; $p < 0.0002$) and *CG14989* (uncharacterized protein; $p = 0.1$) are additional GABA neuron markers. *Gad1*: $p = 0.0005$ (1), $4.42e{-}08$ (2), 0.04 (3), 0.01 (4), and $6.6e{-}08$ (5); *Lim3*: $p = 1.39e{-}05$ (6) and 0.001 (7). *CG14989*, *Lim3*, and *hth* were described as specific markers using single-cell RNA sequencing[41]. The boxes in the gene structures indicate exons and the arrows indicate the transcription direction.

allows simultaneous collection of target nuclei while reducing contamination from non-nuclear DNA. Several studies showed potential cytotoxic effects from GFP overexpression[45,46], though GFP localized using an NLS does not show adverse cellular effects[47]. Additionally, GFP-tagged histone proteins do not perturb chromatin structure[48,49]. Thus, nucleus-specific GFP expression likely has minimal effects and is suitable for ATAC-seq. Further, FANS has good sensitivity and specificity, which increases the likelihood of generating high-quality ATAC-seq libraries from sorted nuclei. While we recovered only few false positive nuclei from GFP-negative flies, even a few false-positive nuclei may present a problem when aiming to sort from Gal4 lines with sparse expression. Sorting at the high-stringency gate will produce fewer false positives but will also reduce the sensitivity for collecting true positives. Possible solutions to the issue of low GFP+ nuclei recovery include increasing the numbers of fly heads, increasing the GFP signal, or using an anti-GFP antibody pulldown method (isolation of nuclei tagged in specific cell types, INTACT)[50,51]. We recommend that specific *Gal4* and *UAS-GFP-nls* combinations be tested to determine GFP+ nuclei recovery prior to performing actual ATAC-seq experiments, particularly for sparsely expressing target neurons.

The *Drosophila* genome is ~tenfold smaller than mammalian genomes, so enzyme-mediated steps during ATAC-seq library preparation may be affected by the amount of available DNA. Tn5 tagmentation in mammalian samples is generally performed using undiluted Tn5 enzyme included in a library preparation kit (1×) for 30 min at 37 °C[37]. Because the amount of accessible chromatin in *Drosophila* nuclei may be lower than in mammalian nuclei, we investigated the effects of changing the parameters of the enzymatic reactions (Tn5 tagmentation and PCR amplification) on fragment distribution and library quality. Previous studies showed that decreasing the Tn5 concentration in mouse embryonic stem cells only decreases tagmentation efficiency when diluted to 10 nM or lower[18]. Notably, this experiment used homemade Tn5[52], which may have different kinetics or concentrations than commercially-available Tn5 enzyme. Increasing the tagmentation time decreased library complexity, while decreasing the tagmentation time increased the number of mid-length fragments but did not improve nucleosomal periodicity. We also examined the number of PCR cycles needed to amplify ATAC-seq libraries before sequencing. Protocols for generating ATAC-seq libraries from mammalian tissues call for amplification to one-third the total fluorescence in a qPCR side reaction[37]. Because of the smaller genome size in *Drosophila*, amplifying ATAC-seq libraries to one-third of the total qPCR fluorescence may introduce GC and size bias. Indeed, amplifying our libraries to one-third qPCR fluorescence introduced a PCR bubble, indicating that the available primers were depleted during amplification[38], causing amplification to occur using annealed adaptor sequences, which increased the mid-size fragments in the library. While these libraries may be sequenceable after one cycle of reconditioning PCR[39], libraries with PCR bubbles should be quality-checked to verify that the PCR bubble was resolved before sequencing. Based on these results, we recommend transposition with 1× Tn5 for 23 min, followed by amplification of the ATAC-seq libraries to 25% qPCR fluorescence, which preserves library complexity and does not introduce GC or size bias. One difference between our optimized protocol and

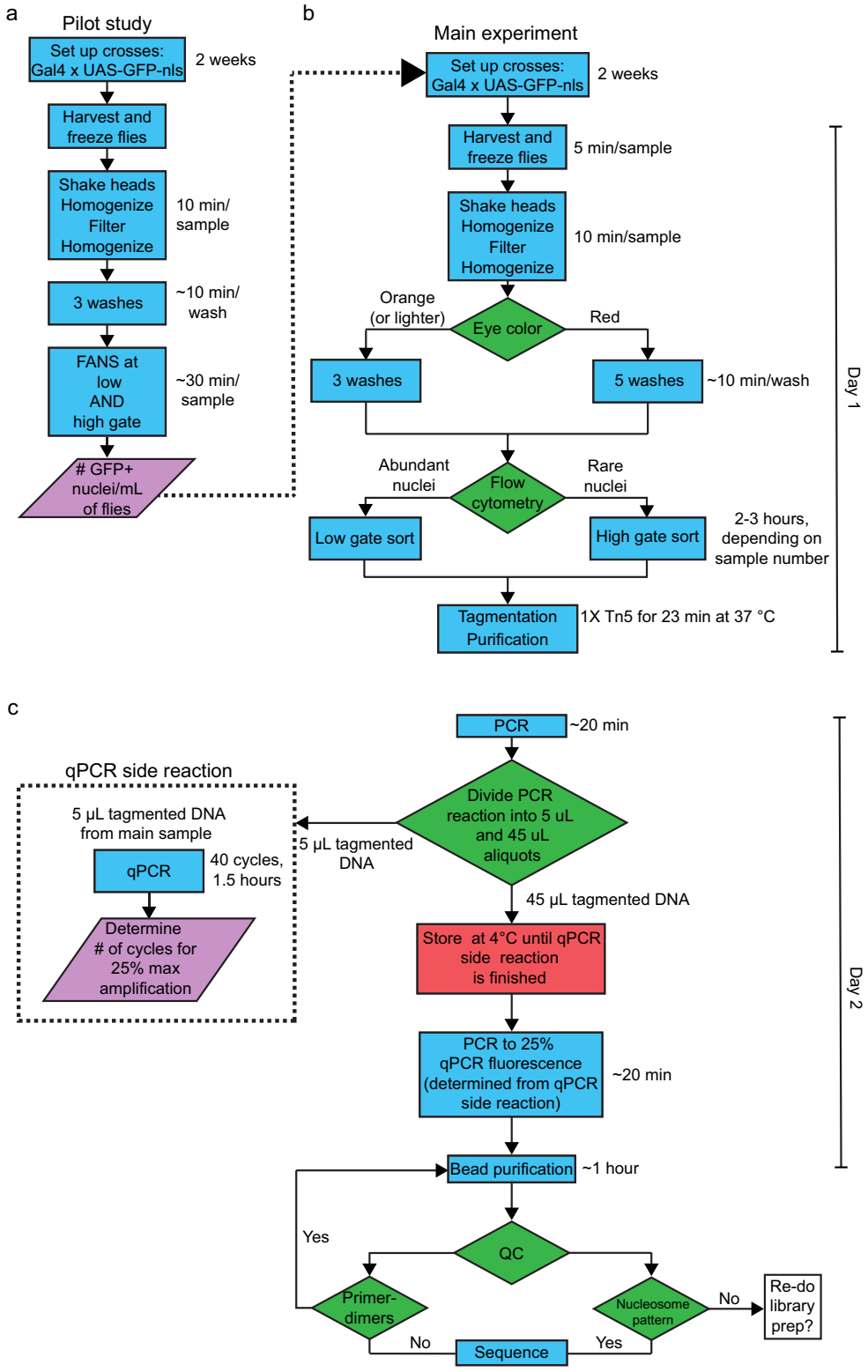

Figure 8. Flow chart of ATAC-seq library preparation from *Drosophila* nuclei. Suggested workflow, which we routinely use to generate ATAC-seq libraries from adult *Drosophila*. The libraries prepared using the workflow conform to ENCODE guidelines, with typical markers indicating a high-quality library, including nucleosomal banding patterns, high genome alignment rates, and high fraction of reads in peaks (FRiP). (**a**) Pilot study to determine inputs and parameters for the main experiment. (**b**) Nuclei isolation and tagmentation reaction. (**c**) Library amplification and purification. In the workflow, blue boxes indicate procedural steps, green diamonds indicate decision points, purple slanted boxes indicate information that inform steps in the main experiment (dotted lines), and the red box indicates a safe stopping point. On the right of each procedural box is shown the approximate time required for each step.

the original ATAC-seq protocol is the enzyme used for PCR amplification. While the Phusion enzyme we used has been previously used for ATAC-seq library preparation[53], the Q5 enzyme listed in the original protocol may be more appropriate for transcription factor footprinting or single nucleotide polymorphism profiling due to its higher fidelity.

Using these optimized conditions, we generated ATAC-seq libraries from 65,000 nuclei isolated from *Drosophila* dopaminergic and GABAergic neurons. These libraries were of high quality, with the expected nucleosomal banding patterns and fragment size distributions. Additionally, these libraries had high alignment rates, further confirming their quality. Therefore, we propose that ATAC-seq libraries from *Drosophila* tissues should use the following parameters (Fig. 8): freezing at − 80 °C for no more than 5 min, at least three washes, 23-min tagmentation time with 1× Tn5, and amplification to 25% qPCR fluorescence. We also suggest that the library quality should be assessed before sequencing via an electrophoresis-based method[37], a qPCR-based method[54,55], or both. This will ensure that the sequenced libraries are high-quality, which will ultimately reduce experimental cost. Our protocol harnesses the powerful genetic tools available in *Drosophila* to achieve excellent cell-type specificity followed by ATAC-seq, which is used to interrogate the chromatin landscape with unprecedented resolution. Thus, our protocol will enable detailed investigations of the role of chromatin-mediated gene regulation in normal and pathological states.

Data availability

The datasets generated by this study are deposited in the GEO database (Accession number: GSE197760).

Received: 19 November 2021; Accepted: 14 March 2022
Published online: 11 April 2022

References

1. Simon, J. M., Giresi, P. G., Davis, I. J. & Lieb, J. D. Using formaldehyde-assisted isolation of regulatory elements (FAIRE) to isolate active regulatory DNA. *Nat. Protoc.* **7**, 256–267 (2012).
2. McKay, D. J. & Lieb, J. D. A common set of DNA regulatory elements shapes Drosophila appendages. *Dev. Cell* **27**, 306–318 (2013).
3. Kidder, B. L., Hu, G. & Zhao, K. ChIP-Seq: Technical considerations for obtaining high-quality data. *Nat. Immunol.* **12**, 918–922 (2011).
4. Cusanovich, D. A. *et al.* Multiplex single cell profiling of chromatin accessibility by combinatorial cellular indexing. *Science* **348**, 910–914 (2015).
5. Buenrostro, J. D. *et al.* Integrated single-cell analysis maps the continuous regulatory landscape of human hematopoietic differentiation. *Cell* **173**, 1535-1548.e16 (2018).
6. Buenrostro, J. D., Giresi, P. G., Zaba, L. C., Chang, H. Y. & Greenleaf, W. J. Transposition of native chromatin for fast and sensitive epigenomic profiling of open chromatin, DNA-binding proteins and nucleosome position. *Nat. Methods* **10**, 1213–1218 (2013).
7. Liu, C. *et al.* An ATAC-seq atlas of chromatin accessibility in mouse tissues. *Sci. Data* **6**, 1–10 (2019).
8. Bysani, M. *et al.* ATAC-seq reveals alterations in open chromatin in pancreatic islets from subjects with type 2 diabetes. *Sci. Rep.* **9**, 1–12 (2019).
9. Davie, K. *et al.* Discovery of transcription factors and regulatory regions driving in vivo tumor development by ATAC-seq and FAIRE-seq open chromatin profiling. *PLoS Genet.* **11**, 1–24 (2015).
10. Lu, Z., Hofmeister, B. T., Vollmers, C., DuBois, R. M. & Schmitz, R. J. Combining ATAC-seq with nuclei sorting for discovery of cis-regulatory regions in plant genomes. *Nucleic Acids Res.* **45**, e41 (2017).
11. Quillien, A. *et al.* Robust identification of developmentally active endothelial enhancers in Zebrafish using FANS-assisted ATAC-Seq. *Cell Rep.* **20**, 709–720 (2017).
12. Halstead, M. M. *et al.* Systematic alteration of ATAC-seq for profiling open chromatin in cryopreserved nuclei preparations from livestock tissues. *Sci. Rep.* **10**, 1–12 (2020).
13. Bozek, M. *et al.* ATAC-seq reveals regional differences in enhancer accessibility during the establishment of spatial coordinates in the Drosophila blastoderm. *Genome Res.* **29**, 771–783 (2019).
14. Haines, J. E. & Eisen, M. B. Patterns of chromatin accessibility along the anterior-posterior axis in the early Drosophila embryo. *PLoS Genet.* **14**, e1007367 (2018).
15. Cusanovich, D. A. *et al.* The cis-regulatory dynamics of embryonic development at single-cell resolution. *Nature* **555**, 538–542 (2018).
16. Brovkina, M. V., Duffié, R., Burtis, A. E. C. & Clowney, E. J. Fruitless decommissions regulatory elements to implement cell-type-specific neuronal masculinization. *PLoS Genet.* **17**, e1009338 (2021).
17. Jenett, A. *et al.* A GAL4-driver line resource for Drosophila neurobiology. *Cell Rep.* **2**, 991–1001 (2012).
18. Corces, M. R. *et al.* An improved ATAC-seq protocol reduces background and enables interrogation of frozen tissues. *Nat. Methods* **14**, 959–962 (2017).
19. Fujiwara, S., Baek, S., Varticovski, L., Kim, S. & Hager, G. L. High quality ATAC-Seq data recovered from cryopreserved breast cell lines and tissue. *Sci. Rep.* **9**, 1–11 (2019).
20. Wang, J. *et al.* ATAC-Seq analysis reveals a widespread decrease of chromatin accessibility in age-related macular degeneration. *Nat. Commun.* **9**, 1–13 (2018).
21. Ho, Y. T. *et al.* Chromatin accessibility identifies diversity in mesenchymal stem cells from different tissue origins. *Sci. Rep.* **8**, 1–11 (2018).
22. Koenecke, N., Johnston, J., Gaertner, B., Natarajan, M. & Zeitlinger, J. Genome-wide identification of Drosophila dorso-ventral enhancers by differential histone acetylation analysis. *Genome Biol.* **17**, 1–19 (2016).
23. Franceschini, N., Kirschfeld, K. & Minke, B. Fluorescence of photoreceptor cells observed in vivo. *Science (80-).* **213**, 1264–1267 (1981).
24. Miller, G. V., Itoku, K. A., Fleischer, A. B. & Stark, W. S. Studies of fluorescence in Drosophila compound eyes: Changes induced by intense light and vitamin A deprivation. *J. Comp. Sens. Y Neural Physiol. A.* **154**, 297–305 (1984).
25. Vinogradov, A. E. Evolution of genome size: Multilevel selection, mutation bias or dynamical chaos?. *Curr. Opin. Genet. Dev.* **14**, 620–626 (2004).
26. Canapa, A., Barucca, M., Biscotti, M. A., Forconi, M. & Olmo, E. Transposons, genome size, and evolutionary insights in animals. *Cytogenet. Genome Res.* **147**, 217–239 (2016).
27. Wolf, F. W., Rodan, A. R., Tsai, L. T. Y. & Heberlein, U. High-resolution analysis of ethanol-induced locomotor stimulation in Drosophila. *J. Neurosci.* **22**, 11035–11044 (2002).

28. Miskimen, K. L. S., Chan, R. & Haines, J. L. Assay for transposase-accessible chromatin using sequencing (ATAC-seq) data analysis. *Curr. Protoc. Hum. Genet.* **2017**, 20.4.1-20.4.13 (2017).
29. Langmead, B. & Salzberg, S. L. Fast gapped-read alignment with Bowtie 2. *Nat. Methods* **9**, 357–359 (2012).
30. Li, H. *et al.* The sequence alignment/map format and SAMtools. *Bioinformatics* **25**, 2078–2079 (2009).
31. Zhang, Y. *et al.* Model-based analysis of ChIP-Seq (MACS). *Genome Biol.* **9**, R137 (2008).
32. Liao, Y., Smyth, G. K. & Shi, W. The R package Rsubread is easier, faster, cheaper and better for alignment and quantification of RNA sequencing reads. *Nucleic Acids Res.* **47**, e47 (2019).
33. Love, M. I., Huber, W. & Anders, S. Moderated estimation of fold change and dispersion for RNA-seq data with DESeq2. *Genome Biol.* **15**, 1–21 (2014).
34. Shariatmadari, R., Sipilä, P. P., Huhtaniemi, I. T. & Poutanen, M. Improved technique for detection of enhanced green fluorescent protein in transgenic mice. *Biotechniques* https://doi.org/10.2144/01306st0630,1282-1285 (2018).
35. Milani, P. *et al.* Cell freezing protocol suitable for ATAC-Seq on motor neurons derived from human induced pluripotent stem cells. *Sci. Rep.* **6**, 1–10 (2016).
36. Ojelade, S. A. *et al.* Rsu1 regulates ethanol consumption in Drosophila and humans. *Proc. Natl. Acad. Sci. U. S. A.* **112**, E4085–E4093 (2015).
37. Buenrostro, J. D., Wu, B., Chang, H. Y. & Greenleaf, W. J. ATAC-seq: A method for assaying chromatin accessibility genome-wide. *Curr. Protoc. Mol. Biol.* **109**, 21.29.1-21.29.9 (2015).
38. Kanagawa, T. Bias and artifacts in multitemplate polymerase chain reactions (PCR). *J. Biosci. Bioeng.* **96**, 317–323 (2003).
39. Thompson, J. R., Marcelino, L. A. & Polz, M. F. Heteroduplexes in mixed-template amplifications: Formation, consequence and elimination by 'reconditioning PCR'. *Nucleic Acids Res.* **30**, 2083–2088 (2002).
40. Davis, C. A. *et al.* The encyclopedia of DNA elements (ENCODE): Data portal update. *Nucleic Acids Res.* **46**, D794–D801 (2018).
41. Davie, K. *et al.* A single-cell transcriptome atlas of the aging Drosophila brain. *Cell* **174**, 982-998.e20 (2018).
42. Allen, A. M. *et al.* A single-cell transcriptomic atlas of the adult Drosophila ventral nerve cord. *Elife* **9**, 1–32 (2020).
43. Rocks, D. *et al.* Cell type-specific chromatin accessibility analysis in the mouse and human brain. *Epigenetics* https://doi.org/10.1080/15592294.2021.1896983 (2021).
44. Deng, B. *et al.* Chemoconnectomics: Mapping chemical transmission in Drosophila. *Neuron* **101**, 876-893.e4 (2019).
45. Ansari, A. M. *et al.* Cellular GFP toxicity and immunogenicity: Potential confounders in in vivo cell tracking experiments. *Stem Cell Rev. Rep.* **12**, 553–559 (2016).
46. Koelsch, K. A., Wang, Y. J., Maier-Moore, J. S., Sawalha, A. H. & Wren, J. D. GFP affects human T cell activation and cytokine production following in vitro stimulation. *PLoS One* **8**, e50068 (2013).
47. Kintaka, R., Makanae, K. & Moriya, H. Cellular growth defects triggered by an overload of protein localization processes. *Sci. Rep.* **6**, 1–11 (2016).
48. Zink, D., Sadoni, N. & Stelzer, E. Visualizing chromatin and chromosomes in living cells. *Methods* **29**, 42–50 (2003).
49. Kanda, T., Sullivan, K. F. & Wahl, G. M. Histone-GFP fusion protein enables sensitive analysis of chromosome dynamics in living mammalian cells. *Curr. Biol.* **8**, 377–385 (1998).
50. Deal, R. B. & Henikoff, S. The INTACT method for cell type-specific gene expression and chromatin profiling in *Arabidopsis thaliana*. *Nat. Protoc.* **6**, 56–68 (2010).
51. Jauregui-Lozano, J., Bakhle, K. & Weake, V. M. In vivo tissue-specific chromatin profiling in *Drosophila melanogaster* using GFP-tagged nuclei. *Genetics* **218**, iyab079 (2021).
52. Picelli, S. *et al.* Tn5 transposase and tagmentation procedures for massively scaled sequencing projects. *Genome Res.* **24**, 2033–2040 (2014).
53. Gambini, A. *et al.* Developmentally programmed tankyrase activity upregulates β-catenin and licenses progression of embryonic genome activation. *Dev. Cell* **53**, 545-560.e7 (2020).
54. Tannenbaum, M. *et al.* Regulatory chromatin landscape in *Arabidopsis thaliana* roots uncovered by coupling INTACT and ATAC-seq. *Plant Methods* **14**, 1–12 (2018).
55. Grbesa, I., Tannenbaum, M., Sarusi-Portuguez, A., Schwartz, M. & Hakim, O. Mapping genome-wide accessible chromatin in primary human T lymphocytes by ATAC-seq. *J. Vis. Exp.* **2017**, 56313 (2017).

Acknowledgements

This work was supported by the University of Utah Flow Cytometry Facility, the University of Utah Genomics Core Facility, the High Throughput Sequencing Core at the Huntsman Cancer Institute, and the National Cancer Institute through Award Number 5P30CA042014-24. The content is solely the responsibility of the authors and does not necessarily represent the official views of the National Institutes of Health.

Author contributions

C.B.M. performed ATAC-seq experiments, analyzed data; and wrote the manuscript; M.A.P. performed nuclei isolation, sorting, and optimization experiments; A.B.M. analyzed data; A.R.R. reviewed and edited the manuscript; A.R. supervised the project and revised and edited the manuscript. All authors reviewed the manuscript.

Funding

This study was supported by grants from the National Institute on Drug Abuse (Grant R21DA049635 to A.R.), the National Institute on Alcohol Abuse and Alcoholism (Grant R01AA026818 to A.R.), and the National Institute of Diabetes and Digestive and Kidney Diseases (R01DK110358 to A.R.R.).

Competing interests

The authors declare no competing interests.

Additional information

Supplementary Information The online version contains supplementary material available at https://doi.org/10.1038/s41598-022-09869-4.

Correspondence and requests for materials should be addressed to C.B.M. or A.R.

Reprints and permissions information is available at www.nature.com/reprints.

Publisher's note Springer Nature remains neutral with regard to jurisdictional claims in published maps and institutional affiliations.